Nuclear Engineering and Technology 52 (2020) 869–877

Contents lists available at ScienceDirect

Nuclear Engineering and Technology

journal homepage: www.elsevier.com/locate/net

Original Article

Physics study for high-performance and very-low-boron APR1400 core with 24-month cycle length

Manseok Do [a, b], Xuan Ha Nguyen [a], Seongdong Jang [a], Yonghee Kim [a, *]

[a] Department of Nuclear and Quantum Engineering, Korea Advanced Institute of Science and Technology (KAIST), 291 Daehak-ro, Yuseong-gu, Daejeon, 34141, Republic of Korea
[b] Nuclear Fuel Design Dept., KEPCO Nuclear Fuel Company Ltd. (KNFC), 242, Daedeok-daero 989 Beon-gil, Yuseong-gu, Daejeon, 34057, Republic of Korea

ARTICLE INFO

Article history:
Received 7 February 2019
Received in revised form
15 August 2019
Accepted 28 October 2019
Available online 31 October 2019

Keywords:
APR1400
Very-low-boron
CSBA
24-month cycle
Serpent
COREDAX

ABSTRACT

A 24-month Advanced Power Reactor 1400 (APR1400) core with a very-low-boron (VLB) concentration has been investigated for an inherently safe and high-performance PWR in this work. To develop a high-performance APR1400 which is able to do the passive frequency control operation, VLB feature is essential. In this paper, the centrally-shielded burnable absorber (CSBA) is utilized for an efficient VLB operation in the 24-month cycle APR1400 core. This innovative design of the VLB APR1400 core includes the optimization of burnable absorber and loading pattern as well as axial cutback for a 24-month cycle operation. In addition to CSBA, an Er-doped guide thimble is also introduced for partial management of the excess reactivity and local peaking factor. To improve the neutron economy of the core, two alternative radial reflectors are adopted in this study, which are SS-304 and ZrO_2. The core reactivity and power distributions for a 2-batch equilibrium cycle are analyzed and compared for each reflector design. Numerical results show that a VLB core can be successfully designed with 24-month cycle and the cycle length is improved significantly with the alternative reflectors. The neutronic analyses are performed using the Monte Carlo Serpent code and 3-D diffusion code COREDAX-2 with the ENDF/B-VII.1.

1. Introduction

The Advanced Power Reactor 1400 (APR1400) is an evolutionary pressurized water reactor (PWR) designed by Korea Electric Power Corporation (KEPCO). The APR1400 system is one of the Generation-III PWRs and generates 1400 MW of electric power [1,2]. There are two units in operation (Shin Kori Units 3&4) and eight units under construction in South Korea and the United Arab Emirates.

APR1400 was originally designed for an 18-month cycle fuel management. A longer fuel cycle with a fixed outage time will yield a higher plant availability, which offsets the increased fuel cycle costs. It also lessens the radiation exposure on the operation and maintenance personnel and improves the "as low as reasonably achievable (ALARA)" design. Extension to 24-month fuel cycle removes one outage in every six-year operating period compared to 18-month fuel cycle. Therefore, the fuel cycle management with refueling interval of 24 months may bring down the total costs. Motivated by these advantages, 24-month cycle designs for various PWRs are gaining more attention recently [3,4].

Extension of cycle length may give negative effects on the plant design and operation. The U-235 enrichment should be increased and accompanying higher initial excess reactivity requires higher concentrations of boron and lithium in the coolant and that makes the water chemistry more costly and harder. It also results in several concerns such as boron-induced corrosion of structures, increased probability of axial offset anomaly (AOA), and a generation of larger amount of liquid waste. Moreover, the moderator temperature coefficient (MTC) is likely to be positive due to a high boron concentration at the beginning of cycle (BOC) during the hot zero power (HZP) and low power operation.

In this paper, a very low boron (VLB) concentration is pursued to achieve two goals. The first goal is to minimize the adverse effects of the soluble boron in the primary system. The second one is to enable APR1400 to do the passive frequency control (PFC) [5], in which active reactivity controls are not required during a frequency control operation. If boron concentration is low enough, a strong negative MTC is secured and the negative MTC can accommodate small moderator temperature changes during a frequency control

* Corresponding author.
E-mail address: yongheekim@kaist.ac.kr (Y. Kim).

https://doi.org/10.1016/j.net.2019.10.020

without any control rod movements. The VLB APR1400 core is called hereinafter APR1400-VLB in this work.

To perform physics studies on the APR1400-VLB core with 24-month cycle length, a Monte Carlo (MC) and diffusion hybrid two-step procedure [6] is utilized in the current work. The Serpent 2 code [7,8] with the Evaluated Nuclear Data Fila ENDF/B-VII.1 library is used for the fuel assembly (FA) lattice calculations and the COREDAX nodal diffusion code [9] is used for 3-D nodal calculations of the APR1400-VLB cores.

2. Design goals and methodology for APR1400-VLB

2.1. Major design features of APR1400

The reactor core of APR1400 is designed to generate 3983 MWth power [1,2]. The active core consists of 241 FAs made of fuel rods containing uranium dioxide fuel. Radial layout of the APR1400 core is depicted in Fig. 1 and Table 1 shows the major design features of the APR1400 core. Each FA consists of a 16 × 16 array of 236 fuel rods and 5 guide thimbles (GTs), as shown in Fig. 2 [1]. In-core instruments are installed in the central instrumentation tubes of selected FAs. The moderator inlet and outlet temperatures are 290.6 °C and 323.9 °C, respectively. In the standard 18-month cycle design, the maximum fuel rod enrichment is 4.5 wt% and gadolinia (Gd_2O_3) admixed with UO_2 is utilized as the burnable absorber (BA) to manage excess reactivity and power profile. The critical boron concentration (CBC) for a typical equilibrium core is about 1250 ppm for unrodded full power operation condition at BOC. In each gadolinia-bearing fuel rod, a low enriched fuel, typically 2.0 wt % U-235 is used and there are top and bottom 6-inch cutbacks, where BA is not applied.

2.2. Design goals

It is presumed that the essential design goals of the standard APR1400 core should be satisfied in the APR1400-VLB pursued in this work. Table 2 lists design basis or design limits relevant to APR1400-VLB core design.

The design limits on the power distribution for APR1400 are determined in terms of peak linear heat generation rate (PLHGR) and required power margin for the minimum departure from nuclear boiling ratio (DNBR). Since the power density and the rated thermal power for APR1400-VLB are the same as in APR1400, the same design limits on the power distribution are assumed in the APR1400-VLB design. The peak fuel rod burnup is usually limited for fuel integrity in the APR1400 core design. In this paper, a new fuel design is adopted for the APR1400-VLB core and there is no clear guidelines regarding the peak fuel burnup. Nevertheless, it is assumed that the current burnup limit for the APR1400 fuel rod is applicable to APR1400-VLB, too. To prevent possible Xe instability or spatial power oscillation in big PWRs, the power shape should be controlled. Extreme saddle shape should be avoided for effective control of any Xe oscillations with control rods. In view of the economy, it is obvious that the fuel discharge burnup should be maximized for a given fuel enrichment and cycle length.

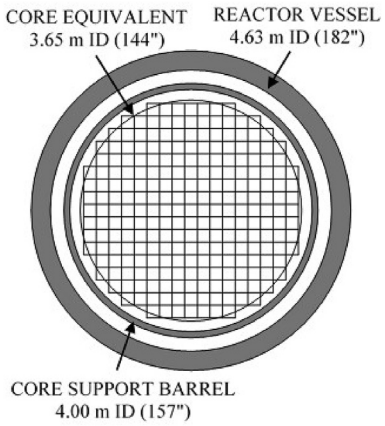

Fig. 1. Cross sectional view of APR1400 core.

Table 1
APR1400 core technical parameters.

Parameter	Value
Thermal power (MWth)	3983
Active core height (cm)	381
Equivalent diameter (cm)	365
Fuel assembly type	16 × 16
Number of fuel assemblies	241
Maximum fuel enrichment (wt%)	4.50
BA cutback (cm)	15.24
Coolant inlet temperature (°C)	290.6

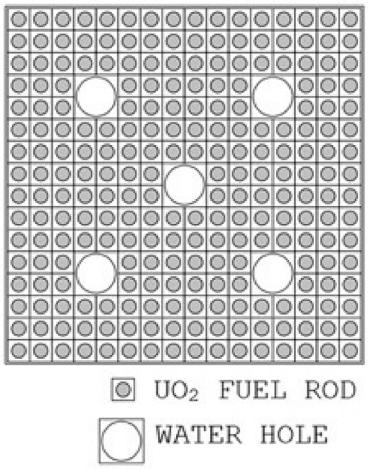

Fig. 2. Typical 16 × 16 CE-type fuel assembly configuration.

To be able to do the PFC operation, the equilibrium APR1400-VLB core should maintain sufficiently low CBC from the BOC condition. It was demonstrated that the PFC is well possible for large-size PWRs if the MTC is below −25 pcm/°C as inlet coolant temperature variation is minimized [10]. Fig. 3 shows MTC vs. boron concentration for a typical 16 × 16 Combustion Engineering (CE)-type FA without BA, where the enrichment of 184 normal fuel pins and 52 low-enriched fuel pins are 4.65 wt% and 4.1 wt%, respectively. The two-dimensional multi-group transport theory code KARMA [11] was used for the MTC calculation at typical moderator and fuel temperatures. Taking into account that the expected core average burnup at BOC is about 12.5 GWD/MTU in the APR1400-VLB core, the maximum CBC of 400 ppm is desirable for a VLB core operation. In this study, however, the targeted maximum CBC during equilibrium cycle is set to 500 ppm, since MTC is expected to be well below −25 pcm/°C except for BOC in the targeted APR1400-VLB core.

2.3. Monte Carlo diffusion hybrid methodology

In this paper, the APR1400-VLB core is analyzed using a MC-diffusion two-step procedure [6]. For the first step, the Monte Carlo Serpent 2 code with nuclear library ENDF/B-VII.1 is used to

Table 2
Design bases for APR1400-VLB equilibrium core.

Parameter	Design Bases or Reference Values
Power distribution	
- Rod-wise radial peak power	1.55[a]
- 3-D heat flux peaking factor	2.43[a]
Maximum fuel rod burnup	<60 GWD/MTU[a]
Power distribution stability	To suppress power distribution oscillation
Least negative MTC	Sufficient for passive frequency control
Maximum critical boron concentration	Low enough for passive frequency control
Cycle length	>670 EFPDs[b]

[a] Typical limits for APR1400.
[b] Effective full power days.

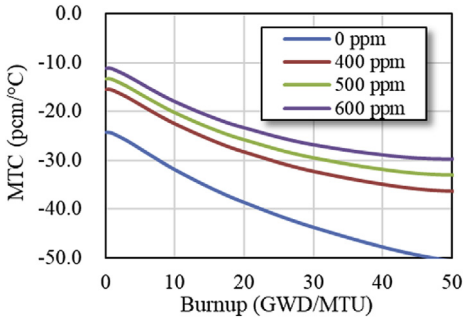

Fig. 3. MTC vs. boron concentration for typical CE-type fuel.

perform the lattice depletion and branch calculations and to obtain homogenized group constants (HGCs) for FAs loaded with the centrally-shielded burnable absorber (CSBA) [12], which is the only BA in the APR1400-VLB core. Advantage of the MC lattice calculation is that CSBA-loaded FAs can be accurately modelled in 3-D geometry while most of the commercial lattice codes are unable to analyze CSBA-loaded FAs. In the Serpent calculations, 500 active and 100 inactive cycles are used with 200,000 histories per cycle. Consequently, the standard deviation of the neutron multiplication factor, k_{eff}, is less than 8.0 pcm and associated uncertainty of two-group HGCs is less than 0.02%. There are a total of 34 burnup points up to 70 GWD/MTU with relatively small burnup intervals in the early depletion steps for accurate modelling of BA depletion, and Xe and Sm buildups. The FA depletion is performed with core average lattice conditions in terms of the specific power, fuel and moderator temperatures, moderator density, and boron concentration. The branch calculations from the reference state are performed at discrete burnups for the four reactor conditions.

In the second step, a 3-D nodal diffusion code, COREDAX, is used for thermal-hydraulic-coupled neutronic analysis of the APR1400-VLB core. The COREDAX code is based on the analytic function expansion nodal (AFEN) [13] method for the neutronic analysis and it has a built-in thermal-hydraulic module which determines the axial temperature profiles for given power profiles in each FA. The standalone COREDAX code is a well proven deterministic code against other commercial codes [9] and Serpent-COREDAX hybrid procedure is also well validated [6]. COREDAX performs so called macroscopic core depletion using the burnup-dependent macroscopic two-group cross sections. The lattice-based homogenized two-group constants and their sensitivity coefficients are tabulated as a function of fuel burnup for the reference core conditions. For each type of group constant, the sensitivity coefficients are evaluated in terms of fuel temperature, moderator temperature, moderator density, and boron concentration. Since the Xe and Sm concentrations depend on actual nodal flux and the boron concentration can be arbitrarily controlled, the microscopic absorption cross section of Xe, Sm, and B-10 is tabulated for the burnup and reactor conditions for the COREDAX analysis. The absorption cross section of node can be determined in the following way:

$$\begin{aligned}\Sigma_a(Bu,T_f,T_m,D_m,S_b) = \Sigma_a^{ref}(Bu) + \frac{\partial\Sigma_a}{\partial\sqrt{T_f}}\Delta\sqrt{T_f} + \frac{\partial\Sigma_a}{\partial T_m}\Delta T_m + \frac{\partial\Sigma_a}{\partial D_m}\Delta D_m + \frac{1}{2}\frac{\partial^2\Sigma_a}{\partial D_m^2}(\Delta D_m)^2 \\ + N_{Hom}^{Xe,\infty}(\varphi_g)\sigma_a^{Xe}(Bu,T_f,T_m,D_m,S_b) \\ + N_{Hom}^{Sm,\infty}(\varphi_g)\sigma_a^{Sm}(Bu,T_f,T_m,D_m,S_b) \\ + N_{Hom}^{B10}(D_m,S_b)\sigma_a^{B10}(Bu,T_f,T_m,D_m,S_b)\end{aligned} \tag{1}$$

$$\begin{aligned}\sigma_a^x(Bu,T_f,T_m,D_m,S_b) = \sigma_a^{x,ref}(Bu) + \frac{\partial\sigma_a^x}{\partial\sqrt{T_f}}\Delta\sqrt{T_f} + \frac{\partial\sigma_a^x}{\partial T_m}\Delta T_m + \frac{\partial\sigma_a^x}{\partial D_m}\Delta D_m \\ + \frac{1}{2}\frac{\partial^2\sigma_a^x}{\partial D_m^2}(\Delta D_m)^2 + \frac{\partial\sigma_a^x}{\partial S_b}\Delta S_b, \quad x = Xe, \ \ Sm, \ \ or\ B10.\end{aligned} \tag{2}$$

where,

Σ_a^{ref} = Ref. macroscopic absorption XS w/o Xe, Sm, and B − 10,
Bu = Burnup,
T_f = Effective Doppler temperature in K,
T_m = Moderator temperature,
D_m = Moderator density,
S_b = Soluble boron concentration,
σ_a^{Xe} = Xe microscopic absorption XS,
σ_a^{Sm} = Sm microscopic absorption XS,
σ_a^{B10} = B − 10 microscopic absorption XS,
$N_{Hom}^{Xe,\infty}(\varphi_g)$ = Xe number density,
$N_{Hom}^{Sm,\infty}(\varphi_g)$ = Sm number density,
$N_{Hom}^{B10}(D_m, S_b)$ = B − 10 number density.

In the current COREDAX analysis for the APR1400 core, two-group constants for baffle-reflector region are determined in the conventional way. First, the Serpent analysis is done for a 1-D spectral geometry, which is composed of FAs, baffle and reflector. From the spectral geometry analysis, the homogenized two-group cross sections and discontinuity factors of the baffle-reflector region are determined.

3. Very low boron APR1400

3.1. Fuel assembly and burnable absorber designs

The conventional gadolinia-bearing fuels used in commercial light water reactors (LWRs) are not very suitable for a VLB core design or extended cycle operation because of their rapid depletion and the consequent large reactivity swing. Also, the homogenous mixture of Gd_2O_3 and UO_2 results in degradation of thermal and mechanical properties of the fuel. Hence, the CSBA is adopted in the APR1400-VLB core design since Gd burning rate can be effectively controlled by adjusting the self-shielding of the CSBA.

In the CSBA concept, Gd_2O_3 balls are loaded in the central region of a typical UO_2 pellet. The unique feature of the CSBA is that it can offer high neutronic flexibility by changing the size and the number of balls in a pellet. Therefore, an optimum depletion pattern which minimizes the excess reactivity and the reactivity swing during operation can be easily achieved with the CSBA design. In the APR1400-VLB design, a less self-shielded 3-ball CSBA is used to accelerate the burning rate of the BA, taking into account the results from CSBA-loaded lattice analyses [12,14]. The 3-ball CSBA concept is illustrated in Fig. 4 and a unit pellet height is assumed to be 1 cm in this analysis. Densities of the CSBA ball and uranium fuel are listed in Table 3. The fabrication feasibility of oxide pellets containing a lumped Gd_2O_3 spherical particle was demonstrated in other study [15].

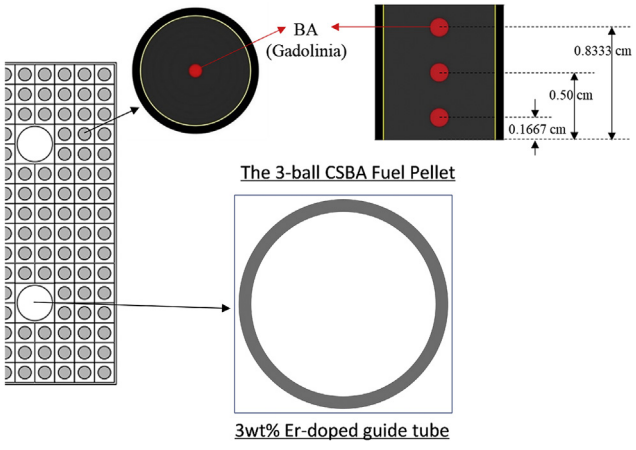

Fig. 4. The 3-ball CSBA fuel rod and Er-doped guide tube.

Table 3
Fuel design features and design parameters for APR1400-VLB.

Parameter	Value
Max. fuel enrichment (wt%)	5.00
CSBA type	3-ball
CSBA cutback (cm)	14.5
Enrichment in cutback region (wt%)	3.00
Fuel stack density (g/cc)	10.313
Gd_2O_3 density (g/cc (%TD))	7.11 (95.95)
Fuel loading scheme	2-batch
No. of feed fuel assemblies	136
Cycle length (EFPD)	670

Since the neutron-absorbing material is loaded in the center of fuel pellet, CSBA is classified as integral type BA. One of the important advantages of the CSBA design is that it remains inside the fuel pellet even in a severe accident scenario. Also, the uranium enrichment is not constrained by CSBA since the gadolinia ball is completely separated from the UO_2 fuel, while typical gadolinia-bearing fuel has a lower enrichment, about 2.0 wt%, due to the thermal conductivity degradation.

Table 3 summarizes fuel design features and core management parameters for APR1400-VLB core. The 3-ball CSBA is included in all fuel locations and the enrichment of the UO_2 pellet is 5.0 wt% with 95.95% theoretical density. The fuel management employs a 2-batch loading scheme and the number of replaced FAs for each cycle is 136.

Table 4 shows three types of CSBA balls loaded in the APR1400-VLB core. The CSBA Type A or Type B with larger Gd_2O_3 balls are placed into inner core regions to reduce fuel depletion rates and power peaking in these regions. On the other hand, CSBA Type C with smaller Gd_2O_3 balls are loaded into peripheral region, where the power density is generally lower. The FA configuration is the same as typical 16 × 16 CE-type fuel as shown in Fig. 2 and there is no radial fuel rod zoning or axial blanket except for axial CSBA cutback. The cutback in APR1400-VLB is 14.5 cm in length for both top and bottom regions of fuel, and plays an important role in flattening axial power distribution.

On the other hand, assembly-wise local peaking factor in a CSBA-loaded FA is a little bit high and the peaking occurs near the large water holes since there is no radial enrichment zoning which is common in commercial designs. Preliminary studies [6,16,17] showed that BA-integrated GTs can be effectively used to manage excess reactivity and to reduce the power peaking near water-holes. In this APR1400-VLB core design, Er-doped GT design is optionally adopted in addition to the CSBA. For the Er-doped GT, a small amount of natural Er is doped in five GTs including the central instrumentation tube. The Er-doped GTs also have top and bottom

Table 4
CSBA types for APR1400-VLB core.

CSBA Type	Type A	Type B	Type C
No. of BA balls	3-ball	3-ball	3-ball
Ball radius (cm)	0.108	0.105	0.088
U-235 wt %	5.00	5.00	5.00

axial cutbacks in the APR1400-VLB design.

3.2. Two-batch fuel management

The proposed loading pattern for APR1400-VLB core is depicted in Fig. 5. In APR1400-VLB design, fresh FAs are divided into three zones (sub-batches) and each fuel zone is loaded with the corresponding CSBA type as described in Table 5. Table 5 also shows the axial CSBA loading for each zone which is necessary in low boron or soluble boron-free core.

In PWRs, MTC is a function of core average boron concentration and the reactivity difference between core top and bottom region is determined by magnitude of MTC. In a VLB core, the axial power is shifted to bottom of the core at BOC because of its highly negative MTC while the power distribution shift is not significant since MTC is barely less than zero at BOC in commercial PWR. As core depletes, the axial power peak moves to top of the core at EOC because core burns faster in bottom region in VLB core. Therefore, the axial CSBA zoning is applied in Zone A to suppress the unbalanced axial power peak and to prevent burnup delay in APR1400-VLB core.

3.3. Alternative reflector designs

To achieve 24-month cycle length, the effective full power day should be 670 days assuming capacity factor of 0.96 and refueling outage of 30 days. Different from the original APR1400 design, materials other than water are considered as radial reflector in APR1400-VLB design to extend the cycle length and to enhance neutron economy. Other advantages of heavy reflector are that it improves long term mechanical behavior of lower internals and it protects reactor vessel against radiation embrittlement. As depict in Fig. 6, the SS-304 or ZrO_2 replaces bypass water between shroud and barrel in APR1400-VLB design. Even though the design of reflector will be complicated to include water channels for cooling or other supporting structures, the solid SS-304 or ZrO_2 are assumed in this study. While only SS-304 reflector is adopted in EPR design [18], the effect of ZrO_2 reflector is also evaluated in this study. As stated in other study [19], zirconium can be more effective as a neutron reflector than iron because it has much lower absorption cross sections and it is much heavier than iron. Since there is possibility that zirconium in reflector region may oxidized under high temperature condition, even rare, the oxidized form of zirconium (ZrO_2) is used as reflector material in APR1400-VLB to remove the risk of damage in reactor system under severe accident.

Table 5
CSBA loading strategies by fuel zone for APR1400-VLB core.

Core Axial Region	CSBA Type		
	Zone A	Zone B	Zone C
Upper half	Type B[a] (Type A)[b]	Type B	Type C
Lower half	Type A	Type B	Type C

[a] Axial CSBA zoning applied in Zone A.
[b] Case without axial zoning for comparison.

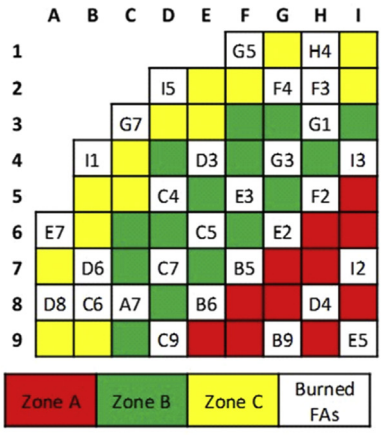

Fuel Location		Fuel Location	
Initial	Reload	Initial	Reload
I5	D2*	F4	G2
I6	-	F6	-
I8	-	E5	I9**
H6	-	D4	H8
H7	-	I1	B4*
G7	C3	I2	I7
I3	I4	G1	H3
H4	H1	F2	H5
G3	G4	E2	G6
G5	F1	E3	F5
F3	H2	D3	E4

* Locations w/o octant symmetry
** Core center location

Fig. 5. The loading pattern for 2-batch APR1400-VLB core.

3.4. Equilibrium cycle analysis

The reactivities calculated for various reflector materials are compared in Table 6 to investigate the neutron economics for each case. This table also compares maximum excess reactivities for BA configurations. As can be seen from the table, the maximum excess reactivities are decreased by about 800 pcm by applying Er-doped GTs. In Table 7, the maximum CBCs and cycle length are compared based on the BA loading configuration and the type of reflector materials. The numerical results show that the cycle length is extended by 14 EFPDs with SS-304 reflector and 18 EFPDs with ZrO_2 reflector. Among heavy reflectors, it is found that ZrO_2-reflected core has slightly longer cycle length, about 4 EFPDs, than SS-reflected core. Fig. 7 shows the boron letdown curves for equilibrium cycle of six APR1400-VLB cores. It is clear that the CBC at BOC are significantly reduced due to the effect of Er-doped GT compared to the cases without Er-doped GT. Meanwhile, previous study [20] showed that the loss in cycle lengths due to CSBA loading is no greater than 30 EFPDs by comparison with the cycle length for BA-free APR1400-VLB core.

To confirm that the APR1400-VLB core is capable of PFC operation, MTC values during the operation are analyzed. The MTC for

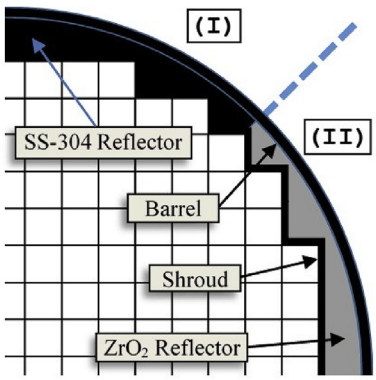

Fig. 6. Alternative SS-304 (I) and ZrO_2 (II) radial reflectors.

Table 6
Comparison of excess reactivities for BA loading configurations and reflector types.

Reflector Material	Excess Reactivity (pcm)		
	Without BA	CSBA only Loaded cor	CSBA with Er-doped GT
Water	-	4205	3398
SS-304	20228	4220	3439
ZrO_2	-	4296	3468

Table 7
Comparison of CBCs and cycle lengths for reflector types with or without Er-doped GT.

Case	Without Er-doped GT		With Er-doped GT	
	Maximum CBC (ppm)	Cycle Length (EFPD)	Maximum CBC (ppm)	Cycle Length (EFPD)
Water-Baffle	613	654	501	651
SS-304	609	667	497	665
ZrO_2	614	673	500	669

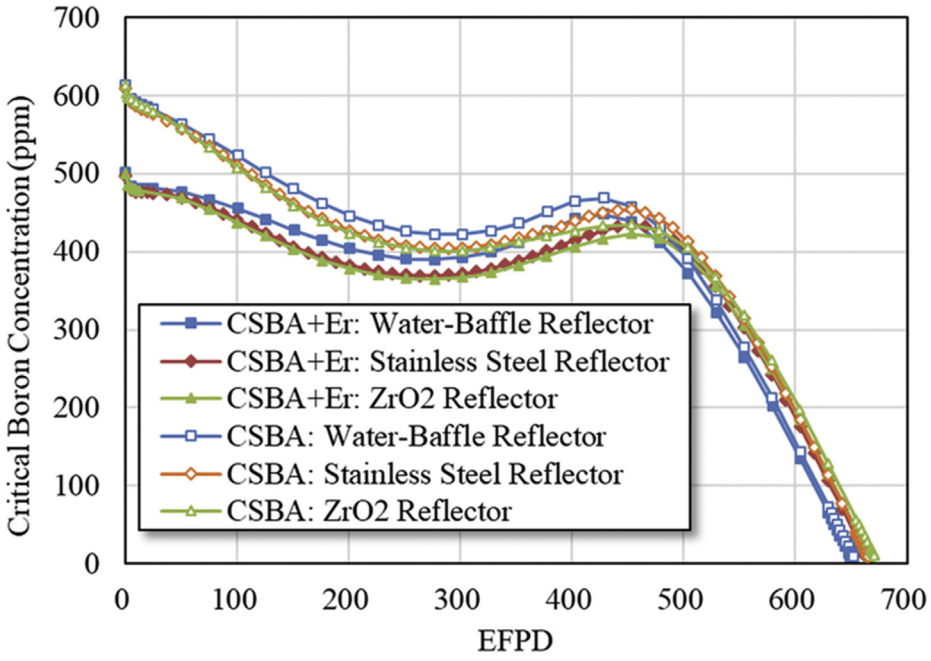

Fig. 7. CBC vs. cycle length for APR1400-VLB core with or without Er-doped GT.

the APR1400-VLB core was evaluated at 500 ppm boron concentration in this study. The evaluated MTC is −35.0 pcm/°C at the BOC condition, where the core average burnup is about 12.5 GWD/MTU. Based on the study in Ref. 10, it is expected that the PFC is possible with the current APR1400-VLB design.

Fig. 8 illustrates normalized radial and axial power profiles at three burnup points for APR1400-VLB core with water, SS-304, and ZrO_2 reflectors. Though Fig. 8 represents the power distributions for the cases with Er-doped GT, the study showed that the power distributions are very similar for cases without Er-doped GT.

Fig. 8 also shows that the relative power in peripheral assemblies increase with heavy reflectors. However, there may exist margin for the loading pattern optimization since the maximum relative powers are not decreased with increasing minimum relative powers with heavy reflectors. The maximum radial assembly power is clearly less than 1.5. Therefore, the radial peak power is estimated to be less than 1.7, which is slightly higher than the limit value in Table 8. However, the 3-D peak power in the APR1400-VLB cores is expected to be within the limit value, 2.43, as the axial peaking factor is about 1.30. It will be possible to reduce the radial peak power below the requirement through core optimization.

Note that the BOC, MOC, and EOC axial power distributions for all reflector types show almost symmetric distribution due to the axial CSBA zoning applied in APR1400-VLB design. As discussed in Section 3.2, the axial CSBA zoning is applied to mitigate axial power shift and the axial power evolutions with and without axial CSBA zoning are compared in Fig. 9 for reference. The comparison model is water-reflected APR1400-VLB core and Er-doped GTs are not applied.

The axial shape index (ASI) at all rod-out (ARO) condition of the APR1400-VLB core at BOC is about 0.062 and it changes to 0.005 at EOC while ASI ranges from about −0.05 to 0.02 during reload cycle of commercial PWRs. The axial power shape of APR1400-VLB core is slightly bottom-skewed at BOC because of its negative MTC,

1.12	1.17	1.22	1.18	1.23	1.20	1.18	1.09	0.64
1.02	1.29	1.17	1.41	1.34	1.02	1.17	1.01	0.56
0.81	1.09	0.91	1.20	1.16	0.87	1.14	1.03	0.64
1.17	1.16	1.18	1.23	1.33	1.24	1.25	0.95	0.53
1.28	1.10	1.39	1.41	1.16	1.25	1.12	0.76	0.43
1.09	0.87	1.17	1.19	0.94	1.15	1.01	0.75	0.47
1.21	1.17	1.23	1.40	1.29	1.16	1.06	0.83	0.54
1.17	1.39	1.41	1.24	1.30	1.00	1.09	0.71	0.49
0.92	1.18	1.18	0.96	1.15	0.94	1.24	0.79	0.61
1.17	1.21	1.38	1.31	1.21	1.13	0.97	0.81	0.35
1.40	1.39	1.22	1.31	1.02	1.19	1.10	0.88	0.34
1.21	1.19	0.96	1.14	0.91	1.29	1.38	1.16	0.45
1.22	1.31	1.27	1.19	1.19	1.15	1.01	0.64	
1.33	1.14	1.28	1.01	1.20	1.03	1.14	0.75	
1.17	0.94	1.15	0.91	1.24	1.07	1.36	1.04	
1.19	1.23	1.15	1.13	1.13	0.97	0.80	0.36	
1.01	1.24	1.00	1.19	1.03	1.09	0.92	0.39	
0.87	1.16	0.93	1.29	1.06	1.34	1.19	0.52	
1.17	1.24	1.05	0.97	1.03	0.82	0.40		
1.17	1.11	1.10	1.12	1.18	0.97	0.45		
1.14	1.01	1.24	1.37	1.36	1.21	0.57		
1.08	0.94	0.83	0.82	0.67	0.45		BOC	
1.00	0.76	0.72	0.91	0.81	0.55		MOC	
1.02	0.75	0.79	1.16	1.07	0.68		EOC	
0.64	0.53	0.54	0.35					
0.56	0.43	0.50	0.35				Max	1.41
0.64	0.47	0.61	0.45				Min	0.34

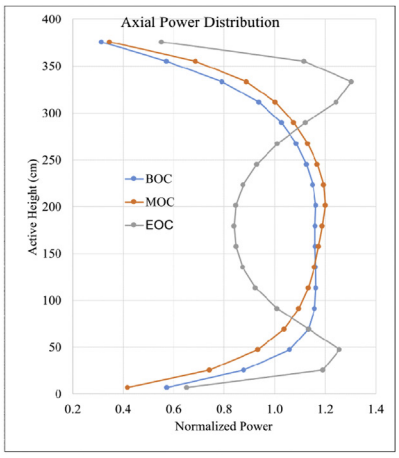

a: Power Distributions for Water Reflected Core

0.98	1.01	1.03	1.02	1.11	1.16	1.22	1.22	0.84
0.90	1.09	0.99	1.18	1.16	0.94	1.12	1.04	0.68
0.95	1.26	1.03	1.35	1.25	0.89	1.12	1.01	0.75
1.00	0.97	1.01	1.06	1.14	1.19	1.30	1.04	0.71
1.09	0.93	1.16	1.18	0.99	1.15	1.04	0.77	0.53
1.26	0.98	1.34	1.32	0.96	1.16	0.94	0.72	0.53
1.03	1.00	1.04	1.15	1.14	1.10	1.10	0.95	0.74
0.99	1.15	1.17	1.03	1.15	0.96	1.12	0.79	0.65
1.04	1.34	1.33	1.00	1.19	0.91	1.17	0.76	0.71
1.01	1.04	1.12	1.12	1.05	1.08	1.02	0.97	0.52
1.17	1.17	1.01	1.14	0.93	1.19	1.21	1.08	0.50
1.36	1.33	0.99	1.19	0.89	1.22	1.27	1.10	0.51
1.09	1.12	1.12	1.04	1.09	1.08	1.10	0.82	
1.15	0.98	1.14	0.92	1.17	1.04	1.33	1.00	
1.26	0.96	1.19	0.88	1.17	0.94	1.22	1.01	
1.15	1.18	1.09	1.08	1.07	1.02	0.94	0.52	
0.94	1.15	0.96	1.20	1.05	1.24	1.16	0.59	
0.89	1.16	0.91	1.21	0.93	1.18	1.07	0.55	
1.22	1.30	1.10	1.03	1.13	0.98	0.58		
1.12	1.04	1.13	1.25	1.39	1.22	0.65		
1.11	0.94	1.16	1.25	1.20	1.07	0.57		
1.21	1.04	0.96	0.99	0.87	0.66		BOC	
1.04	0.77	0.80	1.12	1.08	0.76		MOC	
1.01	0.72	0.75	1.08	1.00	0.65		EOC	
0.84	0.71	0.74	0.54					
0.69	0.54	0.66	0.52				Max	1.39
0.74	0.53	0.70	0.51				Min	0.50

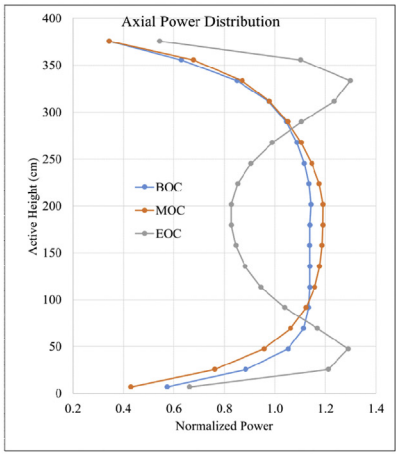

b: Power Distributions for Stainless Steel Reflected Core

0.94	0.97	0.99	0.99	1.08	1.14	1.23	1.24	0.89
0.87	1.05	0.96	1.14	1.13	0.92	1.11	1.04	0.72
0.98	1.30	1.06	1.39	1.27	0.89	1.11	1.00	0.77
0.97	0.93	0.97	1.02	1.10	1.17	1.30	1.06	0.75
1.05	0.90	1.12	1.14	0.96	1.13	1.02	0.77	0.56
1.31	1.01	1.38	1.35	0.97	1.16	0.92	0.71	0.55
0.98	0.96	1.00	1.10	1.11	1.09	1.10	0.97	0.78
0.96	1.11	1.13	0.99	1.12	0.95	1.12	0.80	0.69
1.07	1.38	1.36	1.01	1.20	0.90	1.16	0.75	0.73
0.98	1.00	1.07	1.08	1.02	1.07	1.02	1.00	0.58
1.13	1.13	0.97	1.11	0.91	1.19	1.23	1.11	0.55
1.39	1.36	1.00	1.20	0.88	1.20	1.24	1.08	0.53
1.07	1.08	1.09	1.01	1.07	1.07	1.11	0.86	
1.12	0.95	1.12	0.91	1.16	1.05	1.36	1.05	
1.28	0.97	1.20	0.87	1.15	0.92	1.18	1.00	
1.14	1.17	1.08	1.07	1.06	1.02	0.96	0.57	
0.92	1.13	0.95	1.20	1.05	1.26	1.19	0.64	
0.89	1.16	0.90	1.19	0.90	1.15	1.04	0.55	
1.23	1.30	1.10	1.04	1.14	1.01	0.63		
1.11	1.02	1.14	1.26	1.42	1.25	0.70		
1.11	0.92	1.14	1.22	1.17	1.04	0.57		
1.24	1.06	0.98	1.02	0.92	0.71		BOC	
1.05	0.78	0.81	1.16	1.14	0.80		MOC	
1.00	0.71	0.74	1.06	0.99	0.64		EOC	
0.89	0.76	0.79	0.60					
0.72	0.56	0.70	0.57				Max	1.42
0.76	0.54	0.72	0.52				Min	0.52

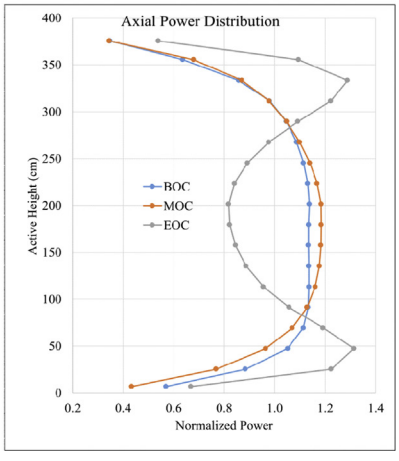

c: Power Distributions for ZrO_2 Reflected Core

Fig. 8. Radial and axial power distributions for APR1400-VLB core.

Table 8
Discharge burnups for APR1400-VLB with CSBA.

Discharge Burnup (GWD/MTU)	Radial Reflector Design		
	Water Refl.	SS Refl.	ZrO_2 Refl.
Average discharge burnup	44.69	46.68	46.93
Average discharge burnup of once burnt FAs	33.32	31.49	31.06
Average discharge burnup of twice burnt FAs	49.34	51.17	51.61
Maximum discharge burnup	57.03	57.54	57.69
Minimum discharge burnup	29.08	30.08	29.71

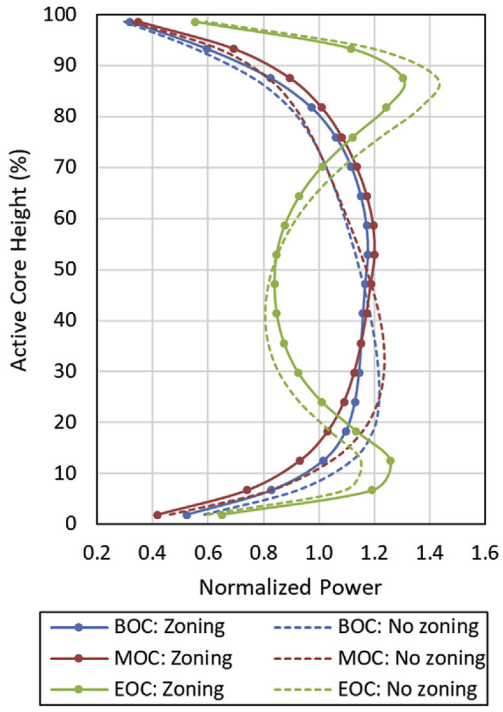

Fig. 9. Axial power distributions: Uniform vs. non-uniform CSBA loading for water-reflected APR1400-VLB.

however, ASIs at MOC and EOC are bounded by the ASI of commercial PWRs. For EOC, the saddle shape is noticeable, but it is similar to saddle shapes at MOC in the initial core of commercial reactors.

Since the axial power shapes with different radial reflector design are very similar as shown in Fig. 8, axial temperature profiles in the case of SS-304 reflector are only depicted in Fig. 10. Obviously, the axial fuel temperature distribution follows axial power shape closely while the coolant temperature distribution at EOC is noticeably different from BOC and MOC due to the saddle power shape. The coolant temperature rise throughout the core is 33.3 °C.

In addition to the power distribution, there are additional constraints regarding burnup in reload design procedure. First, there is a limit with maximum rod average burnup. The maximum discharge burnup and the minimum discharge burnups are summarized in Table 8 for various reflector type. Although the rod average burnup is not evaluated in this paper, it is expected that the maximum rod average burnup will exceed 62 GWD/MTU assuming pin-to-box factor of 1.131 and it is not acceptable in the current state.

On the other hand, discharged assemblies are recommended to satisfy the minimum discharge burnup. The spent fuels are to be stored at Region I or II according to discharge burnup. Spent fuel pool (SFP) Region I is usually used for fresh or partially burnt fuel assemblies and has a storage capacity for one full core, one refueling batch, and five damaged FAs [21]. If the discharge burnup of spent fuel is less than a specific value, that assembly cannot be stored in Region II. Typical minimum burnup requirement for storage in Region II is 35–45 GWD/MTU for 5.0 wt% fuel. For APR1400-VLB, the average discharge burnup of once-burned fuel is 33.3 GWD/MTU, while the average burnup of all discharged fuels are nearly 47 GWD/MTU which is greater than that of 18-month standard APR1400, 44.8 GWD/MTU, due to the higher fuel enrichment.

The local power profiles calculated by Serpent code are compared in Fig. 11 for CSBA-loaded assemblies with and without Er-doped GT. The maximum local powers (pin-to-box factor) at BOC are 1.131 and 1.111 without and with Er-doped GT, respectively. The local peaking factor is quite low compared to that of commercial FAs, considering that there is no radial zoning in the CSBA-loaded assembly. Since the pin peaking factor is found at fuel rods neighboring with large water holes, it can be reduced by applying Er-doped GTs as shown in Fig. 11. It is noted that the associated uncertainty of the pin power is less than 0.15%.

It should be mentioned that the primary shutdown strategy of the standard APR1400 is applicable to the APR1400-VLB core due to following reasons: 1) the control rod design is identical, 2) the core excess reactivity is smaller at BOC condition, and 3) the MTC values for both standard APR1400 and APR1400-VLB are similar and highly negative at EOC condition. As a result, it can be mentioned that the APR1400-VLB core has a sufficient shutdown margin.

4. Conclusions and recommendations

A neutronic investigation on the conceptual design of 24-month cycle APR1400-VLB core loaded with CSBA is presented in this paper, utilizing the MC-diffusion hybrid two-step procedure. The proposed fuel management for APR1400-VLB equilibrium core is 2-batch cycle scheme and replaces 136 FAs for each outage to attain 24-month cycle length. The numerical results show that the power distributions during normal operation are acceptable and the extremely low boron operation is feasible with 24-month cycle length. It is concluded that the highly reliable PFC will be attainable with APR1400-VLB conceptual design by maintaining sufficiently negative MTC from the BOC. This paper also demonstrated that the use of heavy reflector increases the cycle length by at least 14 EFPDs compared with the water-reflected core.

The fuel cycle management with the refueling intervals of 24 months is advantageous since it yields a higher plant availability and may bring down the total cost. The CSBA-loaded APR1400-VLB core design enables the cycle length extension without compromising reactor performances, while minimizing the adverse effects of the soluble boron.

For future work, further design optimization is required to increase the cycle length and fuel discharge burnup. Also, major safety parameters need to be evaluated and compared with those of the existing design.

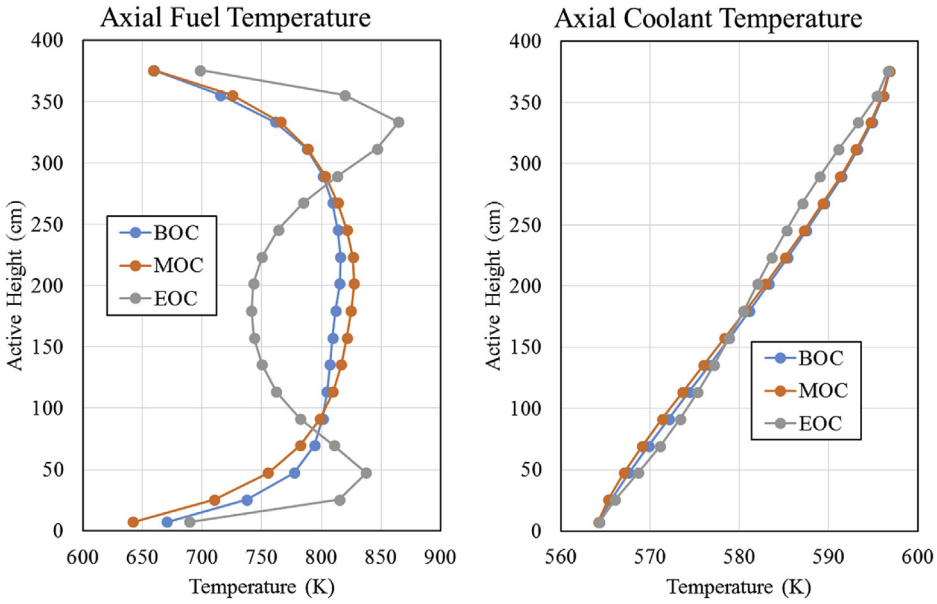

Fig. 10. Core average fuel and modertor temperature distribution for SS-Reflected APR1400-VLB.

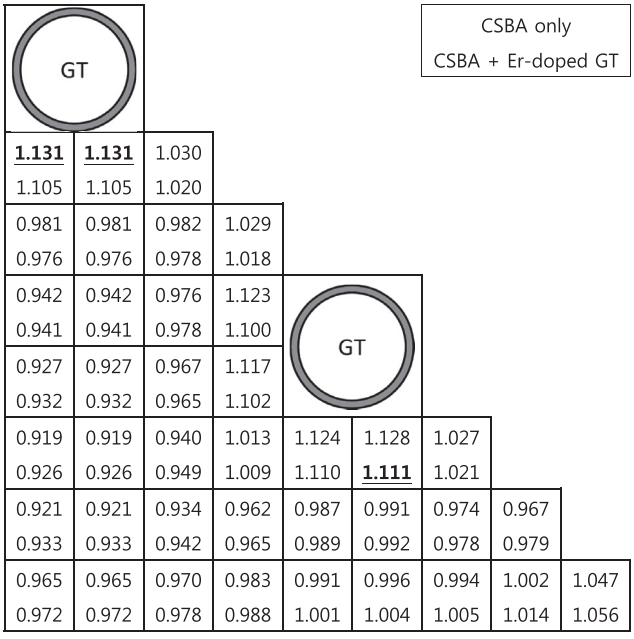

1.131	**1.131**	1.030						
1.105	1.105	1.020						
0.981	0.981	0.982	1.029					
0.976	0.976	0.978	1.018					
0.942	0.942	0.976	1.123					
0.941	0.941	0.978	1.100					
0.927	0.927	0.967	1.117					
0.932	0.932	0.965	1.102					
0.919	0.919	0.940	1.013	1.124	1.128	1.027		
0.926	0.926	0.949	1.009	1.110	**1.111**	1.021		
0.921	0.921	0.934	0.962	0.987	0.991	0.974	0.967	
0.933	0.933	0.942	0.965	0.989	0.992	0.978	0.979	
0.965	0.965	0.970	0.983	0.991	0.996	0.994	1.002	1.047
0.972	0.972	0.978	0.988	1.001	1.004	1.005	1.014	1.056

Fig. 11. Local power distribution for Zone B (r_{CSBA} = 0.105 cm) assembly at 0 GWD/MTU.

Acknowledgement

This research was supported by the National Research Foundation of Korea (NRF) Grant funded by the Korean Government (MSIT) (NRF-2016R1A5A1013919).

References

[1] APR1400 design control document and environmental report. https://www.nrc.gov/reactors/new-reactors/design-cert/apr1400/dcd.html.
[2] Status Report 83 - Advanced Power Reactor 1400 MWe (APR1400), 2011. https://aris.iaea.org/PDF/APR1400.pdf.
[3] S. Jeong, H. Jun, S. Shon, S. Moon, H. Shin, Feasibility study on 24 month cycle scheme for OPR1000 PWR, in: Pacific Basin Nuclear Conference, San Francisco, USA, September 30-October 4, 2018.
[4] S. Son, J. Lee, et al., Preliminary evaluation of the hybrid long-term cycle strategy for PWR in Korea, in: Fourth International Conference on Nuclear Power Plant Life Management, Lyon, France, October 23-27, 2017.
[5] A.E. Abdelhameed, X.H. Nguyen, Y. Kim, Feasibility of passive autonomous frequency control operation in a Soluble-Boron-Free small PWR, Ann. Nucl. Energy 116 (2018) 319–333.
[6] M.S. Yahya, Y. Kim, An innovative core design for a soluble-boron-free small pressurized water reactor, Int. J. Energy Res. (2017) 1–9.
[7] J. Leppänen, M. Pusa, T. Viitanen, V. Valtavirta, T. Kaltiaisenaho, The Serpent Monte Carlo code: status, development and applications in 2013, Ann. Nucl. Energy 82 (2015 August) 142–150.
[8] J. Leppänen, Serpent A Continuous Energy Monte Carlo Reactor Physics Burn-Up Calculation Code, VTT Technical Research Centre of Finland, Espoo, Finland, 2013.
[9] B. Cho, S. Yuk, N.Z. Cho, Y. Kim, User's Manual for the Rectangular Three-dimensional Diffusion Nodal Code COREDAX-2 Version 1.8, ROK: KAIST, 2016. Report no. NURAPT-2016-01.
[10] A.E. Abdelhameed, J. Lee, Y. Kim, Physics conditions of passive autonomous frequency control operation in conventional large-size PWRs, Prog. Nucl. Energy 118 (2020).
[11] KARMA User's Manual, KNF-TR-CDT-13021 Rev. 2, KEPCO Nuclear Fuel Co., June 2015.
[12] X.H. Nguyen, A.A.E. Abdelhameed, Y. Kim, Optimization of centrally shielded burnable absorbers in soluble-boron-free SMR design, in: Transactions of the Korean Nuclear Society Autumn Meeting, Gyeongju, Korea, October 25-27, 2017.
[13] J.M. Noh, N.Z. Cho, A new approach of analytic basis function expansion to neutron diffusion nodal calculation, Nucl. Sci. Eng. 116 (165) (1994).
[14] X.H. Nguyen, C.H. Kim, Y. Kim, An advanced core design for a soluble-boron-free small modular reactor ATOM with centrally-shielded burnable absorber, Nucl. Eng. Technol. (2018), https://doi.org/10.1016/j.net.2018.10.016. Available online.
[15] Mistarihi, et al., Fabrication of oxide pellets containing lumped Gd_2O_3 using Y_2O_3-stabilized ZrO_2 for burnable absorber fuel applications, Int. J. Energy Res. (42) (2018) 2141–2151.
[16] M. Yahya, H. Yu, Y. Kim, Burnable absorber-integrated Guide Thimble (BigT) – I: design concepts and neutronic characterization on the fuel assembly benchmarks, J. Nucl. Sci. Technol. 53 (7) (2015) 1048–1060, https://doi.org/10.1080/00223131.2015.1090937.
[17] M. Yahya, Y. Kim, Burnable absorber-integrated guide thimble (BigT) – II: application to 3D PWR core design, J. Nucl. Sci. Technol. 53 (10) (2016) 1521–1527, https://doi.org/10.1080/00223131.2015.1129367.
[18] Framatome ANP, Inc, EPR Design Description, 2005.
[19] J. Choe, D. Lee, J. Jung, H.C. Shin, Performance evaluation of Zircaloy reflector for pressurized water reactors, Int. J. Energy Res. 40 (2) (2015) 160–167, https://doi.org/10.1002/er.3443.
[20] M. Do, X.H. Nguyen, Y. Kim, Design of a very-low-boron APR1400 core with 24-month cycle length using centrally-shielded burnable absorber, in: Proceedings of NURER 2018," Jeju, Korea, September 30-October 3, 2018.
[21] KEPCO & KHNP, Criticality Analysis of New and Spent Fuel Storage Racks, November 2014. APR1400-Z-A-NR-14011-NP, Rev.0.